The autocorrelation function of stellar p-mode measurements and its diagnostic properties

Ian W. Roxburgh, Sergei Vorontsov

Mon. Not. R. Astron. Soc. **369,** 1491–1496 (2006) doi:10.1111/j.1365-2966.2006.10396.x

The autocorrelation function of stellar p-mode measurements and its diagnostic properties

I. W. Roxburgh[1,2★] and S. V. Vorontsov[1,3]

[1]*Astronomy Unit, Queen Mary, University of London, Mile End Road, London E1 4NS*
[2]*LESIA, Observatoire de Paris, Place Jules Janssen, 92195 Meudon, France*
[3]*Institute of Physics of the Earth, B. Gruzinskaya 10, Moscow 123810, Russia*

Accepted 2006 March 27. Received 2006 February 28

ABSTRACT

The basic properties of acoustic wave propagation in stellar interiors can be analysed from the autocorrelation function (ACF) of intensity (or velocity) observations without measuring the resonant p-mode frequencies. We show how the strength of acoustic wave refraction in the stellar core, or forward acoustic amplitude, can be measured from a modulation in the ACF. This is the basic physical quantity which governs the so-called 'small frequency separations', and its measurement from the ACF can be used for determining the small frequency separations when the data is of insufficient quality for a reliable identification of the stellar p-mode frequencies.

Key words: methods: numerical – stars: oscillations.

1 INTRODUCTION

In stellar seismology, the diagnostic potential of observational data on solar-like stars is usually attributed solely to frequency measurements. However, the reliable determination of p-mode frequencies from power spectra of intensity (or Doppler velocity) observations is known to be a difficult task, especially for distant stars, since the amplitudes of the stochastically excited acoustic modes are very small. Having an alternative analysis technique is thus highly desirable.

The autocorrelation function (ACF) of the observational time-string (or, alternatively, the power spectrum of the power spectrum) provides an obvious and robust way of estimating the average value of the frequency spacings between modes of consecutive radial order, the so-called 'large frequency separations'; this quantity gives a measure of the stellar acoustic diameter. In this paper, we analyse the diagnostic properties of the ACF in further detail and show how it can be used to evaluate the average value of 'small frequency separations' – the quantity which measures the strength of acoustic wave refraction in the stellar core.

In solar seismology, the ACF of whole-disc measurements has been used in a number of studies (Grec et al. 1997; Fossat et al. 1999). When analysing the ACF of *SOHO* GOLF measurements, Gabriel et al. (1998) were the first to consider in detail a prominent modulation of the peak amplitudes in the ACF on a time-scale short compared with mode lifetimes. A similar modulation, seen in *SOHO* MDI data, is shown in Fig. 1. Even peaks (time delays a multiple of 4 h) decrease rapidly with higher time delays, while odd peaks begin to show up, and become larger than even peaks; later on they show beating. Using numerical modelling of the ACF, this modulation was (correctly) attributed by Gabriel et al. (1998) to deviations of the p-mode frequencies from simplest first-order asymptotic prediction of uniform frequency spacings. Our analysis is aimed essentially at understanding the origin of this effect.

Section 2 contains a simple physical interpretation of the ACF in terms of acoustic wavepacket propagation; it shows that the rate of modulation gives a measure of the forward acoustic amplitude. In Section 3, we recall the results of classical analysis of stellar p modes (Roxburgh & Vorontsov 2000) linking the concepts of forward action and forward amplitudes with the large and small frequency separations. An analysis in terms of spherical harmonic (p-mode) expansion is described in Section 4. In Section 5, we consider the basic properties of sensitivity coefficients of whole-disc measurements relevant to our analysis, and in Section 6 we discuss the diagnostic value of the resulting description.

2 PHYSICAL DESCRIPTION

Consider the evolution of a single non-dispersive wavepacket emitted at time $t = 0$ by a point-like source located somewhere near the stellar surface (Fig. 2). We assume that the packet propagates without dissipation or scattering in the stellar interior, and suffers multiple reflections without energy loss from the stellar surface. The wavepacket contributes to the observational signal when it meets the surface. To discuss the contribution to the observational time-string, it is convenient to start with an artificial experiment where the star is observed simultaneously from all the directions. In other words, let us imagine first that the signal (brightness or vertical velocity) is averaged over the entire stellar surface.

2.1 'Whole-star' measurements

The propagation of the wavepacket in the stellar interior is accompanied by a wave travelling along the stellar surface, which contributes

★E-mail: I.W.Roxburgh@qmul.ac.uk

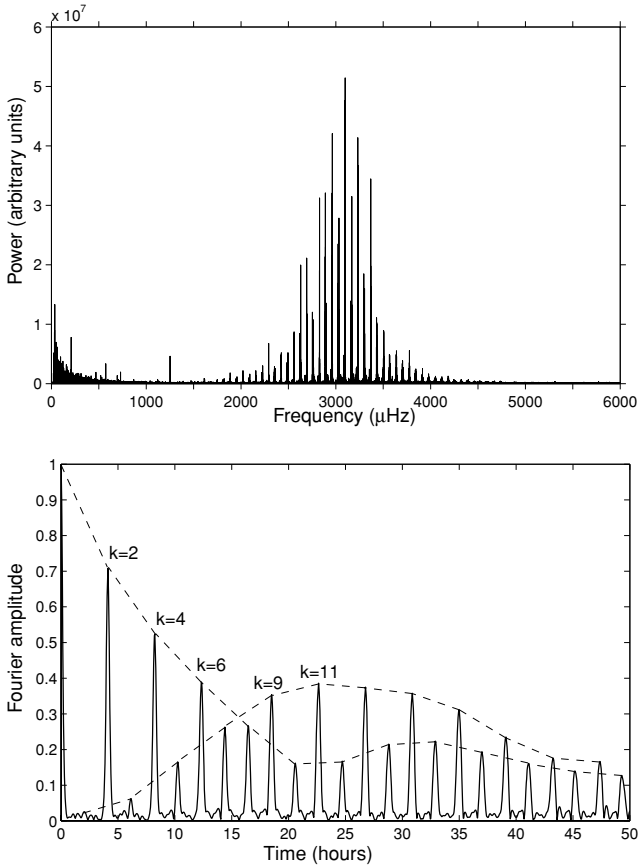

Figure 1. Top: power spectrum of 1 yr of solar Doppler velocity measurements with *SOHO* MDI, targeted at $l = 0$ modes (velocity averaged over the solar disc). Bottom: amplitude of the Fourier transform of the power spectrum, multiplied by a cosine window between 1.5 and 4.5 mHz. We employ the Fourier amplitude, which is the envelope of the ACF, to suppress the rapid (5-min) oscillations in the ACF. The dashed lines show the envelope of $k =$ even and $k =$ odd peaks.

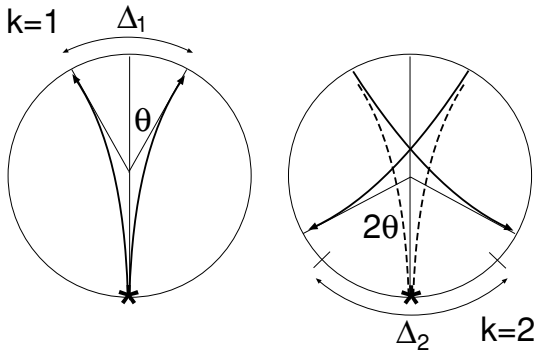

Figure 2. First ($k = 1$) and second ($k = 2$) transits of an acoustic wave through the stellar interior.

a small oscillatory signal to the observational time-string, until the packet arrives at the point on the surface diametrically opposite to the excitation source. This will happen at time $t = 2T$, where T is the stellar acoustic radius (the sound wave propagation time between the centre and the surface). This first arrival ($k = 1$) of the wave travelling directly along the stellar diameter will produce a strong peak in the observational time-string. We now introduce the action $S(\theta)$ as the phase integral in the direct acoustic wave between the source and the point on the opposite hemisphere specified by deflection angle θ (Fig. 2). The amplitude of the peak in the observational time-string is governed by the signal received from a small circular area in the vicinity of the stationary point $\theta = 0$ of $S(\theta)$. The angular size θ_1 of this coherence domain is such that action S varies by $\pi/2$ from its forward value at $\theta = 0$:

$$(1 - \cos\theta_1)\left(\frac{\partial S}{\partial \cos\theta}\right)_{\theta=0} = \frac{\pi}{2}. \tag{1}$$

The size of the coherence domain as measured by the solid angle $\Delta_1 = 2\pi\,(1 - \cos\theta_1)$ is

$$\Delta_1 = \pi^2 \left(\frac{\partial S}{\partial \cos\theta}\right)^{-1}_{\theta=0}. \tag{2}$$

After the second transit through the star ($k = 2$), the action S along any acoustic ray is twice as large and the deflection angle θ (now measured from the source) is also twice as large, hence $(\partial S/\partial \cos\theta)_{\theta=0}$ is twice as small. We then have $1 - \cos\theta_2$ twice as large as $1 - \cos\theta_1$, and hence $\Delta_2 = 2\Delta_1$. After k transits, we will get

$$\Delta_k = k\pi^2 \left(\frac{\partial S}{\partial \cos\theta}\right)^{-1}_{\theta=0}. \tag{3}$$

Since the acoustic wave amplitude at consecutive stationary points varies with k as $1/k$, the peaks in the observational time-string will occur at a regular interval $2T$ with constant amplitude. The ACF will look similar to the time-string itself; it corresponds to an oscillation power spectrum which consists of spectral lines separated in frequency ω by $(2T)^{-1}$. These are radial modes, excited by the source; indeed, our artificial 'whole-star' measurements are only sensitive to $l = 0$ modes.

2.2 'Whole-disc' measurements

We now turn to the realistic situation when only half the stellar surface is visible, and start with the simplest geometry, where the excitation source is located at the centre of the visible hemisphere. The first transit through the star goes to the invisible side and will not be detected. At small k, only $k =$ even transits will enter the time-string. But as k increases, the size of the coherence domain grows linearly with k (equation 3), and even signals will start to decrease in amplitude when the coherence domain extends beyond the visible hemisphere. Simultaneously, $k =$ odd signals will appear as their coherence domain in the far side of the star extends to the front side and becomes visible. We expect that signals of even and odd transits will become equal in magnitude when the coherence domain fills the complete solid angle, $\Delta_k \simeq 4\pi$, which will happen when

$$k_{\text{even}=\text{odd}} \simeq \frac{4}{\pi}\left(\frac{\partial S}{\partial \cos\theta}\right)_{\theta=0}. \tag{4}$$

As k increases further, the amplitudes of even signals will continue to decrease, and signals with $k =$ odd will continue to increase, until the coherence domain covers about three halves of the stellar surface, $\Delta_k \simeq 6\pi$. We thus expect the even signals to reach their minimum amplitudes, and odd signals their maximum amplitudes when

$$k_{\text{minmax}} \simeq \frac{3}{2}k_{\text{even=odd}} \simeq \frac{6}{\pi}\left(\frac{\partial S}{\partial \cos\theta}\right)_{\theta=0}. \tag{5}$$

At higher k, we expect both even and odd signals to show periodic variation with k with nearly the same amplitude, but with opposite phase. If the wavepacket loses a small part of its energy on each reflection (or when propagating inside the star), the amplitudes in the time-string, and in the ACF, will show a slow exponential decay at large k.

Our initial assumption about the source location (at the centre of visible hemisphere) can now be lifted. When the source is at the stellar limb, the first even and odd signals will all come with the same amplitude, but this amplitude is small (due to foreshortening, limb darkening, line-of-sight projection in velocity measurements). When the source moves closer to the disc centre (or to the diametrically opposite point at the far side of the star), the amplitudes will increase, and will show the modulation described above.

The quantity $(\partial S/\partial \cos\theta)_{\theta=0}$ in equations (4) and (5) is inversely proportional to the forward acoustic wave amplitude (Roxburgh & Vorontsov 2000). It measures the widening of a thin acoustic flux tube centred at the stellar diameter, caused by wave refraction in the stellar core. Equations (4) and (5) can be used for evaluating this quantity directly from the ACF. From *SOHO* MDI data shown in Fig. 1, we infer $k_{\rm even=odd} \simeq 7.5$ and $k_{\rm minmax} \simeq 11$.

This is a simplest possible description. It does not take into account the non-uniform sensitivity of the observations to signals coming from different locations on the visible stellar hemisphere. In particular, we can expect $k_{\rm even=odd}$ and $k_{\rm minmax}$ to have somewhat different values in velocity and intensity measurements, since an effective 'sensitivity' domain is smaller in velocity due to line-of-sight projection. A more sophisticated description thus calls for an expansion of both the signal and the sensitivity function in spherical harmonics; this will be given in Section 4.

3 RELATION WITH SMALL FREQUENCY SEPARATIONS

In the classical approximation (where acoustic waves propagate in the stellar interior along well-defined rays without any partial reflection or scattering), the oscillation frequencies, $\omega_{n,l}$, of low-degree high-frequency p modes of order of n and degree l are given by the eigenfrequency equation (Roxburgh & Vorontsov 2000)

$$\omega T + \delta_0(\omega) + l(l+1)D_\delta(\omega) \simeq \pi\left[n + \frac{l}{2} + \frac{1}{4} + \alpha_{\rm out}(\omega)\right]. \quad (6)$$

Here, $\delta_0(\omega)$ is the internal phase shift for modes of degree $l = 0$ and $\alpha_{\rm out}(\omega)$ is the surface phase shift; both quantities are of the order of 1 in magnitude. T is the stellar acoustic radius, and $l(l+1)D_\delta$ is the first degree dependent term in the expansion of the internal phase shift in powers of $l(l+1)$, with

$$D_\delta = \frac{1}{4}\left(\frac{\partial S}{\partial \cos\theta}\right)^{-1}_{\theta=0}, \quad (7)$$

which is a measure of the forward amplitude.

Neglecting the slow variation of $\delta_0(\omega)$ and $\alpha_{\rm out}(\omega)$ with frequency ω, the large separations are

$$\Delta\omega = \omega_{n+1,l} - \omega_{n,l} \simeq 2\pi\left(\frac{\partial S}{\partial\omega}\right)^{-1}_{\theta=0} \simeq 2\pi(2T)^{-1}, \quad (8)$$

and the ratio of small to large frequency separations is

$$\frac{\omega_{n,\ell} - \omega_{n-1,\ell+2}}{\omega_{n+1,\ell} - \omega_{n,\ell}} \simeq \frac{2(2l+3)}{\pi} D_\delta. \quad (9)$$

For a forward ray ($\theta = 0$) we have $S \simeq 2\omega T$, and the two observable quantities which govern the frequency spacings thus have a simple physical interpretation: the large frequency separation is a measure of the forward action, and the ratio of small to large separations measures the forward amplitude. Equations (7) and (9) allow one to interpret $k_{\rm even=odd}$ and $k_{\rm minmax}$ in the ACF in terms of the small frequency separations.

4 SPHERICAL HARMONIC (p-MODE) EXPANSION

We now use the p-mode representation of the power spectrum to incorporate the non-uniform sensitivity of whole-disc observations to modes of different degree, taking the sensitivity coefficients (in power) for modes of degree l be a_l. (We assume that for $l > 3$ the a_l are sufficiently small to be neglected.) Instead of working with the ACF, which is the cosine Fourier transform of the two-sided power spectrum (positive and negative ω), it is more convenient to model the amplitude of the complex Fourier transform of the one-sided power spectrum (positive ω), which gives the envelope of the rapidly oscillating ACF.

Consider a set of four neighbouring modes of degree $l = 0$–3 with frequencies $\omega_{n,0}, \omega_{n,1}, \omega_{n-1,2}, \omega_{n-1,3}$, which we designate as $\omega_l, l = 0, 1, 2, 3$. In the classical approximation their frequencies are given by equations (6), (8) and (9) as

$$\omega_0 = n\Delta\omega + \Omega, \quad \omega_1 = \omega_0 + \frac{\Delta\omega}{2\pi}(\pi - \varphi),$$
$$\omega_2 = \omega_0 - \frac{\Delta\omega}{2\pi}3\varphi, \; \omega_3 = \omega_0 + \frac{\Delta\omega}{2\pi}(\pi - 6\varphi), \quad (10)$$

where

$$\Omega = \frac{1}{T}\left(\pi\alpha_{\rm out} + \frac{\pi}{4} - \delta_0\right) \quad \text{and} \quad \varphi = 4D_\delta. \quad (11)$$

Assuming that these four modes with similar frequencies are excited to the same amplitude A_n (the mode masses are nearly the same at low degree and the energy input varies slowly with frequency), and neglecting damping so that the line profiles are Dirac δ functions, $A_n\delta(\omega - \omega_l)$, their contribution to the Fourier spectrum of the power spectrum at time t is

$$\mathrm{d}F(t) = \sum_{l=0}^{l=3}\int_0^\infty A_n\,\delta(\omega-\omega_l)\,a_l\,\mathrm{e}^{\mathrm{i}\omega_l t}\,\mathrm{d}\omega = A_n\sum_{l=0}^{l=3} a_l\,\mathrm{e}^{\mathrm{i}\omega_l t}, \quad (12)$$

where the a_l are the sensitivity coefficients for whole disc measurements.

At time $t = 2kT = 2k\,\pi/\Delta\omega$ this reduces to

$$\mathrm{d}F_k = A_n\mathrm{e}^{-\mathrm{i}\Omega t}\left[a_0 + a_1 e^{ik(\pi-\varphi)} + a_2 e^{-3ik\varphi} + a_3 e^{ik(\pi-6\varphi)}\right]. \quad (13)$$

We now add up the contribution from all such sets of neighbouring modes each with amplitudes A_n which can vary with frequency and, to within a normalization constant, obtain

$$F_k = a_0 + a_1\mathrm{e}^{\mathrm{i}k(\pi-\varphi)} + a_2\mathrm{e}^{-3\mathrm{i}k\varphi} + a_3\mathrm{e}^{\mathrm{i}k(\pi-6\varphi)}. \quad (14)$$

We now evaluate the difference between $|F_k|^2$ for two consecutive values of k; this difference will be zero at $k = k_{\rm even=odd}$, and will reach its maximum value at $k = k_{\rm minmax}$. With φ small compared to 1 (otherwise the small frequency separations will not be small compared with large separations), it is straightforward to show that

$$|F_{k+1}|^2 - |F_k|^2 \simeq -4(-1)^k a_0 a_1 \times\left[\cos k\varphi + \frac{a_2}{a_0}\cos 2k\varphi + a_3 a_1\left(\frac{a_2}{a_0}\cos 3k\varphi + \cos 6k\varphi\right)\right]. \quad (15)$$

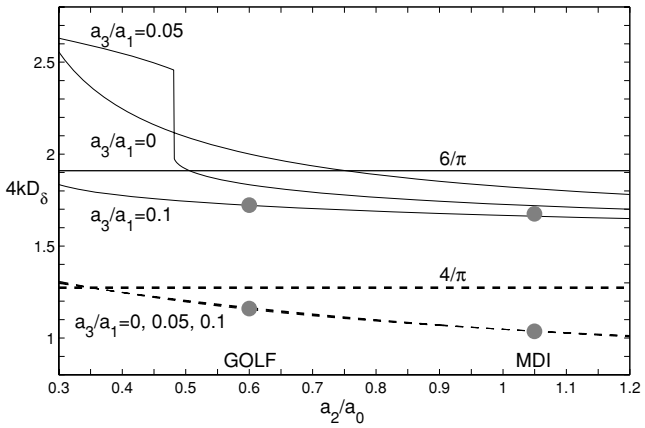

Figure 3. Diagnostic diagram for measuring D_δ from $k_{\rm even=odd}$ and $k_{\rm minmax}$ when the observational sensitivity coefficients $a_0 - a_3$ are known. Solid curves show $4k_{\rm minmax}\, D_\delta$, for three values of a_3/a_0. Dashed curves show $4k_{\rm even=odd}\, D_\delta$; three separate curves cannot be distinguished on the scale of the figure. The two horizontal lines at $4k_{\rm minmax}\, D_\delta = 6/\pi$ and $4k_{\rm even=odd}\, D_\delta = 4/\pi$ are the result of the simple physical description (Section 2). The two grey circles at $a_2/a_0 = 1.05$ indicate the measurement of the solar D_δ with *SOHO* MDI data. The two circles at $a_2/a_0 = 0.60$ are for similar measurement but with data from *SOHO* GOLF, with sensitivity coefficients taken from the numerical fit to the GOLF ACF by Gabriel et al. (1998).

If a_3 is negligibly small (i.e. $l = 3$ modes are discarded in the power spectrum), we get

$$4k_{\rm even=odd} D_\delta \simeq \arccos \frac{1}{4}\left[\sqrt{\left(\frac{a_0}{a_2}\right)^2 + 8} - \frac{a_0}{a_2}\right], \tag{16}$$

$$4k_{\rm minmax} D_\delta \simeq \arccos\left(-\frac{1}{4}\frac{a_0}{a_2}\right) \quad (\text{when } a_3 = 0). \tag{17}$$

For $a_0 > 4a_2$ the right-hand side of the last equation switches to the solution π. Extending the analysis to include $l = 3$ modes requires numerical computation; the results are shown in Fig. 3.

Fig. 3 shows that for the same star, the values of $k_{\rm even=odd}$ and $k_{\rm minmax}$ decrease monotonically when a_2/a_0 increases. This variation, however, is rather small; in the expected range of a_2/a_0, it is within about 20 per cent. We consider this variation as moderate, because what we are targeting is an approximate measurement of an average value of $D_\delta(\omega)$ or small frequency separations (both decrease with frequency) over a frequency interval where the stellar p modes have their largest amplitudes.

We also observe from Fig. 3 that $k_{\rm minmax}$ is much more sensitive to a_3/a_1, as compared to $k_{\rm even=odd}$; at smaller values of a_2/a_0 it suffers rapid transitions from one solution to another. We also expect $k_{\rm minmax}$ to be more sensitive to mode damping, which was not included in the analysis (we have just assumed that the linewidths are small compared to small frequency separations). Energy losses lead to an exponential decay of the ACF with time, and can shift $k_{\rm minmax}$ to a slightly smaller value; the value of $k_{\rm even=odd}$ does not suffer from this effect. Since at larger k the ACF is also expected to be more sensitive to noise in the input data, we conclude that measurement with $k_{\rm even=odd}$ should produce better results. We also observe from Fig. 3 that the simple physical description in terms of wavepacket propagation is in good agreement with more sophisticated p-mode expansion analysis.

The solar values of D_δ decrease with frequency from about 0.045 at 2 mHz, to 0.035 at 3 mHz, and 0.028 at 4 mHz (the small frequency separations between $l = 0$ and 2 modes decrease correspondingly from about 11.5 μHz to 9.0 μHz and 7.3 μHz). Measurements with *SOHO* MDI data shown in Fig. 1, with MDI sensitivities $a_2/a_0 = 1.05$ and $a_3/a_1 = 0.08$, produces $k_{\rm minmax} \simeq 11$, which gives $D_\delta \simeq 0.038$, and $k_{\rm even=odd} \simeq 7.5$, which gives $D_\delta \simeq 0.035$ (the exact value at central frequency of 3 mHz). The simple physical description provides, correspondingly, $D_\delta \simeq 0.043$ and 0.042. Similar measurement with *SOHO* GOLF data (using the ACF shown in fig. 1 of Gabriel et al. 1998) and their fitted values $a_2/a_2 = 0.60$ and $a_3/a_1 = 0.10$ gives $k_{\rm minmax} \simeq 12$ (and hence $D_\delta \simeq 0.036$) and $k_{\rm even=odd} \simeq 8$ (which gives the same value $D_\delta \simeq 0.036$).

Measurements with MDI data can be expected to be more accurate because the sensitivity coefficients are known with better accuracy [we used sensitivity coefficients resulting from leakage matrix calculations described in Vorontsov & Jefferies (2005)].

5 SENSITIVITY COEFFICIENTS

In this section we consider the basic properties of sensitivity coefficients, which are relevant to our analysis. Let us choose spherical coordinates (θ, ϕ) on the stellar surface such that the colatitude θ is measured from the z axis taken as pointing towards the observer. In these coordinates only $m = 0$ modes, described by zonal spherical harmonics

$$Y_{l0}(\theta, \phi) = \left(\frac{2l+1}{4\pi}\right)^{1/2} P_l(\cos\theta), \tag{18}$$

where $P_l(\cos\theta)$ is Legendre polynomial, enter the observation if the sensitivity function, which describes the response to the observational signals coming from different locations on the stellar surface, is axially symmetric. If this sensitivity function is $s(\theta)$, the (amplitude) response coefficient c_l to a p mode of degree l is

$$\begin{aligned} c_l &= \int_{4\pi} s(\theta) Y_{l0}(\theta, \phi)\, {\rm d}\Omega \\ &= \pi^{1/2}(2l+1)^{1/2} \int_0^{\pi/2} s(\theta) P_l(\cos\theta) \sin\theta\, {\rm d}\theta. \end{aligned} \tag{19}$$

The upper limit of the integral on the right-hand side is $\pi/2$ because the sensitivity function is non-zero only in the visible hemisphere.

The coefficients c_l are just the expansion coefficients of $s(\theta)$ in spherical harmonics, a result which is easily obtained by setting $s(\theta) = \sum s_k Y_{k0}(\theta, \phi)$ and integrating over the entire sphere so that

$$c_l = \int_{4\pi} \sum_{k=0}^{\infty} s_k\, Y_{k0}(\theta, \phi)\, Y_{l0}(\theta, \phi)\, {\rm d}\Omega = s_l, \tag{20}$$

since the spherical harmonics are orthogonal and normalized to unity. On integrating $s^2(\theta)$ over the entire sphere and using the orthogonality properties of spherical harmonics we obtain

$$\sum_{l=0}^{\infty} c_l^2 = \int_{4\pi} s^2(\theta)\, {\rm d}\Omega = 2\pi \int_0^{\pi/2} s^2(\theta) \sin\theta\, {\rm d}\theta, \tag{21}$$

where again we have used the fact that $s(\theta)$ is only non-zero in the visible hemisphere.

Now Legendre polynomials have the orthogonality property

$$\int_0^{\pi} P_{l'}(\cos\theta) P_l(\cos\theta) \sin\theta\, {\rm d}\theta = \frac{2}{2l+1}\delta_{l'l}. \tag{22}$$

So, since $P_l(\cos\theta)$ is an even function of $\cos\theta$ when l is even, and odd when l is odd, all the even polynomials are orthogonal to each other on the half-interval $0 \leqslant \theta \leqslant \pi/2$, and the same is true for odd polynomials. In the half-interval $0 \leqslant \theta \leqslant \pi/2$, even and odd polynomials thus form two separate (and complete) orthogonal basis sets:

$$\int_0^{\pi/2} P_{l'}(\cos\theta) P_l(\cos\theta) \sin\theta \, \mathrm{d}\theta = \frac{1}{2l+1}\delta_{l'l}, \quad l'+l = \text{even} \tag{23}$$

The sensitivity function $s(\theta)$, which only differs from zero in the half-interval, can thus be expanded in either even, or odd polynomials (the situation is similar to using either sine or cosine Fourier transform on a finite interval), and we have

$$\sum_{l=\text{even}} c_l^2 = \sum_{l=\text{odd}} c_l^2 = \frac{1}{2}\int_{4\pi} s^2(\theta)\, \mathrm{d}\Omega. \tag{24}$$

For the response coefficients in power, $a_l = c_l^2$, we have

$$\sum_{l=\text{even}} a_l = \sum_{l=\text{odd}} a_l. \tag{25}$$

With $\varphi \ll 1$ and $k = 1$, this relation and equation (14) give $F_1 \simeq 0$. This is the origin the negligible amplitude of the $k = 1$ peak in the ACF, when the ACF is considered in the framework of p-mode expansion.

If another orientation of the coordinate system, (θ', ϕ') is preferred (e.g. for considering effects of stellar rotation), then for each particular mode of degree l and azimuthal order m in the new coordinate system, its spherical harmonic $Y_{lm}(\theta', \phi')$ is a linear combination of $Y_{lm'}(\theta, \phi)$ with $-l \leqslant m' \leqslant l$, and only the $m' = 0$ component of this decomposition will enter the observations. Considering all the possible m states, a new set of sensitivity coefficients c'_{lm} will be related with c_l by the transformation coefficients of $Y_{l0}(\theta, \phi)$ under the rotation of the coordinate system [coefficients of expansion of $Y_{l0}(\theta, \phi)$ into linear combination of $Y_{lm}(\theta', \phi')$], and we have

$$\sum_{m=-l}^{l} {c'_{lm}}^2 = c_l^2 \tag{26}$$

with the individual coefficients c'_{lm} given by the addition theorem for Legendre polynomials. In the present work, we assume that rotational (or magnetic) frequency splittings are small compared to small frequency separations. Individual m states do not correlate in the observational signal (the excitation source is assumed to be random in angular coordinates), and simply add up in the power spectrum to a single $a_l = c_l^2$ given by equation (26).

The simplest form of the sensitivity function is $s(\theta) = \cos\theta$, which accounts for the foreshortening (area projection); it corresponds to intensity measurements with zero limb darkening. It gives sensitivity coefficients $a_2/a_0 = 5/16$, $a_1/a_0 = 4/3$, and $a_3 = 0$. These values are lower limits for any sensitivity function of the form $s(\theta) = f(\theta)\cos\theta$, where f is a monotonically increasing function of $\cos\theta$, as is the case for limb darkening, and the line-of-sight projection in velocity measurements (see Appendix A). The lower limit $a_2/a_0 \simeq 0.3$, was used to limit the horizontal scale in Fig. 3.

6 DISCUSSION

Fig. 4 illustrates an artificial measurement similar to those described above, but when the *SOHO* MDI power spectrum shown in Fig. 1 was distorted by adding noise, of an amplitude which makes the excess power around 3 mHz invisible, and p-mode identification practically impossible. As can be seen from the lower panel, the amplitude of the Fourier transform is closely similar to the corresponding result in Fig. 1, and both the large and the small frequency separations can be determined from the ACF. In this artificial measurement the value of $k_{\text{even=odd}} \simeq 7.5$, the same as in Fig. 1, giving the same value for the averaged small separations.

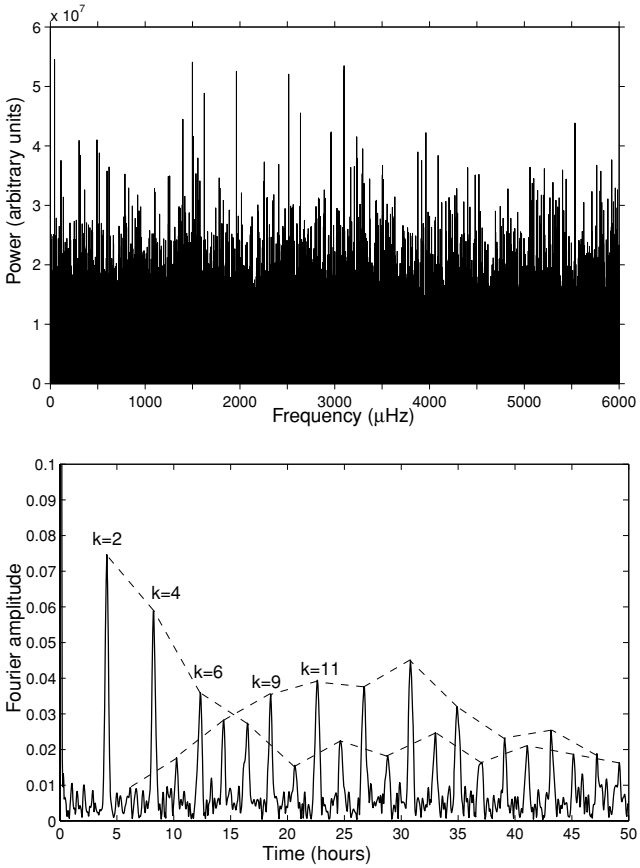

Figure 4. Top: the *SOHO* MDI power spectrum as in Fig. 1, but with added exponentially distributed noise (χ^2 with two degrees of freedom) with a frequency-independent expectation value of 0.25×10^7. Bottom: amplitude of the Fourier transform of the power spectrum, convolved with a cosine window between 1.5 and 4.5 mHz. The dashed lines show the envelope of $k =$ even and $k =$ odd peaks.

Employing the ACF instead of (or in addition to) frequency measurements provides an alternative method of data analysis. Applying the integral transform (Fourier transform) to the power spectrum efficiently suppresses the rapidly varying noisy component, while still allowing a measurement of the average basic parameters which govern acoustic wave resonances in the stellar interior (forward action and forward amplitude), and hence the large and small separations.

Since the approach is very cheap computationally, it can also be particularly productive as a means of initial data analysis in observations with multiple target stars, as in the forthcoming *COROT* mission (Baglin et al. 2002).

We emphasize that the analysis of this paper is only applicable when the classical approximation is relevant, i.e. when acoustic waves propagate through the stellar core without noticeable reflection or scattering, at least in the frequency range of observable p modes. Otherwise, the picture will become more complicated. Reflection of the direct wave by the stellar core, for example, is capable of producing a $k \simeq 1$ signal in the ACF. Answering the question of

whether or not such a reflection is detectable in real stars requires further studies.

ACKNOWLEDGMENTS

We thank J. Schou for providing us with *SOHO* MDI power spectrum which was used in the analysis. *SOHO* is a project of international cooperation between ESA and NASA. This work was supported by the UK PPARC under grant PPA/G/S/2003/00137.

REFERENCES

Baglin A. et al., (the COROT Team), 2002, in Favata F., Roxburgh F., Galadi D., eds, ESA SP-485, Stellar Structure and Habitable Planet Finding. ESA Publications Division, Noordwijk, p. 17

Fossat E. et al., 1999, A&A, 343, 608

Gabriel M., Grec G., Renaud C., Gabriel A. H., Robillot J. M., Roca Cortes T., Turck-Chieze S., Ulrich R. K., 1998, A&A, 338, 1109

Grec G. et al., 1997, in Provost J., Schmider F.-X., eds, Sonding Solar and Stellar Interiors. Kluwer, Dordrecht, p. 91

Roxburgh I. W., Vorontsov S. V., 2000, MNRAS, 317, 141

Vorontsov S. V., Jefferies S. M., 2005, ApJ, 623, 1202

APPENDIX A: LOWER LMITS ON THE SENSITIVITY COEFFICIENTS a_1/a_0

The sensitivity coefficients $a_l = c_l^2$, where the amplitude response coefficients c_l are defined by (cf. equation 18)

$$c_l = \sqrt{(2l+1)\,\pi}\int_0^1 s(x)\,P_l(x)\,\mathrm{d}x, \quad x = \cos\theta. \tag{A1}$$

We consider the case where $s(x) = xf(x)$, where $f(x)$ is a monotonically increasing function of x so $\mathrm{d}f/\mathrm{d}x \geqslant 0$. Now

$$I_k = \int_0^1 x^k f(x)\,\mathrm{d}x = \frac{f(1)}{k+1} - \frac{1}{k+1}\int_0^1 x^{k+1}\frac{\mathrm{d}f}{\mathrm{d}x}\,\mathrm{d}x \tag{A2}$$

or

$$(k+1)\,I_k = f(1) - \int_0^1 x^{k+1}\frac{\mathrm{d}f}{\mathrm{d}x}\,\mathrm{d}x. \tag{A3}$$

Since $\mathrm{d}f/\mathrm{d}x \geqslant 0$ and $x^{k+1} < x^k$ in the interval $0 < x < 1$, it follows that

$$(k+1)\,I_k \geqslant k\,I_{k-1}. \tag{A4}$$

As $P_0(x) = 1, P_1(x) = x, P_2(x) = (3x^2 - 1)/2$, we have

$$c_0 = \sqrt{\pi}\,I_1, \quad c_1 = \sqrt{3\,\pi}\,I_2, \quad c_2 = \sqrt{5\,\pi}\,\frac{(3\,I_3 - I_1)}{2}. \tag{A5}$$

Using the ordering in equation (30) this gives

$$c_1 \geqslant \frac{2}{3}\sqrt{3}\,c_0, \quad c_2 \geqslant \frac{\sqrt{5}}{4}\,c_0 \quad \text{hence} \quad \frac{a_1}{a_0} \geqslant \frac{4}{3}, \quad \frac{a_2}{a_0} \geqslant \frac{5}{16}. \tag{A6}$$

The lower limits corresponding to $f(x) =$ constant.

This paper has been typeset from a TEX/LATEX file prepared by the author.